

A Novel Wideband Microstrip Patch Antenna with Nonuniform Feed Based on Model Predictive

Maryam Farahani and Sajad Mohammad-Ali-Nezhad*

Abstract—A novel wideband microstrip patch antenna with nonuniform transmission line feed is presented using model predictive control. Nonlinear model predictive control (NMPC) is used to achieve a nonuniform transmission line that matches with the microstrip patch antenna. The transmission line is extended using cosine expansion with the impedance differential equation then being used as the dynamic NMPC equation to find the unknown coefficients of that cosine expansion. The transmission line is designed such that the impedance of the input port matches the impedance of the microstrip antenna at the resonance frequency and its adjacent frequencies. The proposed antenna's impedance is 5.15–5.85 GHz. In this bandwidth, the radiation pattern is stable; the cross polarization and back lobe are -30 dB and -20 dB, respectively. The error in the impedance bandwidth is about 4.2%. The simulation and measurement results are considered satisfactory.

1. INTRODUCTION

Microstrip patch antennas have been extensively considered by researchers in recent decades due to their small structure, simple fabrication, low weight, and simplicity of integration with printed circuit elements [1–3]. With the development of modern communication systems in recent years, expansive studies have been conducted to increase the bandwidth of microstrip patch antennas along with characteristics such as low profile and cross polarization [3, 4]. Various techniques like adding a parasitic strip around the radiative element [5, 6], creating a slot in the patch [7, 8], differential-feed [9, 10], increasing the thickness of the substrate and stacking [11], and exciting different radiation modes [13–15] are presented for increasing said bandwidth. However, they have some disadvantages such as a resulting increase of cross polarization, destabilization of the radiation pattern, and increase in the substrate's thickness.

In [5], two U-shaped parasitic elements were inserted around a microstrip patch antenna to increase its impedance bandwidth. However, the size and thickness of the antenna were significant as the antenna's area and thickness were $1.3\lambda_g^2$ and $0.17\lambda_g$, respectively. A wideband microstrip patch antenna with two parasitic mushroom-type arrays with an area of $2.78\lambda_g^2$ was presented in [6]. The use of parasitic elements made the antenna larger and destabilized the radiation pattern. In [7], the elimination of a U-shaped slot from a microstrip antenna increased the bandwidth, but the antenna's thickness was $0.06\lambda_g$. A wideband structure of a patch antenna with a thickness of $0.12\lambda_g$ and a U-shaped slot eliminated was presented in [8]. However, the antenna was made larger and two-layered to achieve a suitable bandwidth. If the thickness of an antenna is low, an unwanted non-radiative mode is activated in the antenna when a slot is eliminated. One method of increasing the impedance bandwidth is based on supply feed. In [9], a differential-feed was used to increase the bandwidth. With this method, it is very difficult to design a low-thickness structure, thus resulting in a substrate thickness of $0.05\lambda_g$. An

Received 27 November 2019, Accepted 11 January 2020, Scheduled 31 January 2020

* Corresponding author: Sajad Mohammad-Ali-Nezhad (s.mohammadalinezhad@qom.ac.ir).

The authors are with the Electrical & Electronics Department, University of Qom, Qom, Iran.

L-probe fed inverted EE-H shaped slotted microstrip patch antenna was introduced in [10]. The use of this feed made the thickness of the antenna $0.11\lambda_g$ and the cross-polarization 10 dB at some frequencies.

Another method of increasing the impedance bandwidth is to increase thickness and stacking, which enlarges the antenna. Therefore, such an antenna may not be suitable for some new applications which require a low thickness [11]. Also, a defected ground structure was employed in [12] to make circular ring microstrip wideband. Variation in the antenna ground made the back lobe approximately 5 dB. Yet another technique to increase the impedance bandwidth of a microstrip patch antenna is to excite several radiative resonance modes. In [13], two modes were excited by placing a shorting pin in the triangular microstrip patch, thus increasing the bandwidth. However, the resulting substrate thickness was $0.09\lambda_g$, and the antenna's area increased to approximately 2.9, thus becoming somewhat large. Two radiation modes were excited in an aperture-coupled microstrip patch antenna in [14], and moreover, the antenna's bandwidth was 15. However, the side lobe level of the E -plane radiation pattern increased. A dual-mode wideband circular sector patch antenna was then proposed in [15]; however, the antenna's gain was not stable on the broadside.

Most of recent works have been even concentrated on the real impedance matching, or they have suffered from a large length [16]. Also researches which have used NTLs for complex impedance matching had some disadvantages such as low bandwidth or large dimensions [17].

In contrast, NMPC specifically implements the problem constraints, thus it can be simply formulated and finally, be solved issues with a standard software as a constrained optimization problem, so the NMPC method is faster and more accurate. The purpose of this study is to increase a microstrip antenna's bandwidth with a nonuniform feed line. Since the line's equation exists, and it is possible to write the equation in a form of state space by using NMPC, it is possible to recommend a suitable feeding line with high accuracy and speed. In recent years, using NMPC has been one of the key strategies in control systems and process industries such as chemical plants, power electronics, ventilation, and air conditioning (HVAC) System Energy Efficiency [18, 19].

In this paper, a wideband inset feed microstrip patch antenna with low cross polarization and a substrate thickness of $0.02\lambda_g$ is produced by using a proposed nonuniform transmission line to match the antenna with a coaxial cable. Impedance of the microstrip patch antenna is calculated using HFSS. In order to match the input port, a transmission line that changes its width trigonometrically is proposed. Suitable coefficients to achieve the optimal impedances at different frequencies are calculated using NMPC. The antenna has an impedance bandwidth of 5.15–5.85 GHz and cross polarization of -30 dB, and the simulation results and measurement results are satisfactory. The impedance of the microstrip patch antenna and expansion of the non-uniform microstrip line are presented in Section 2. In Section 3, the transformation of the differential equation of the output impedance variation of the transmission line into a state-space equation is shown. Moreover, a suitable nonuniform feed line is designed using NMPC to match the microstrip patch antenna. Section 4 provides the simulation results of the proposed antenna obtained from HFSS along with the measurement results. The simulation results are in good agreement with the measurement ones.

2. DESIGN OF THE ANTENNA USING MPC

A microstrip patch antenna has a low bandwidth because its impedance variations in single mode at different frequencies are very large. Also, the impedance of the patch at one frequency is real whilst having a small real part and a significant imaginary part at other frequencies. Since the transmission line from the coaxial cable to the patch antenna has real impedance, the transmission line and microstrip antenna cannot be matched except at the resonance frequency. To this aim, a nonuniform transmission line can be used which has a real impedance at the central frequency while its impedance values at adjacent frequencies around its excited mode are complex values close to the value of the antenna's impedance. In order to design the transmission line, the width of line should be extended using cosine coefficients. Then, the differential equation of the transmission line's impedance is solved using NMPC. Finally, the proper unknown coefficients for obtaining the desired impedance of the transmission line are extracted.

Figure 1 shows the proposed microstrip patch antenna with the nonuniform transmission line. The substrate is Roger 4003 with a thickness of 0.8 mm and loss tangent of 0.02. The antenna's dimensions

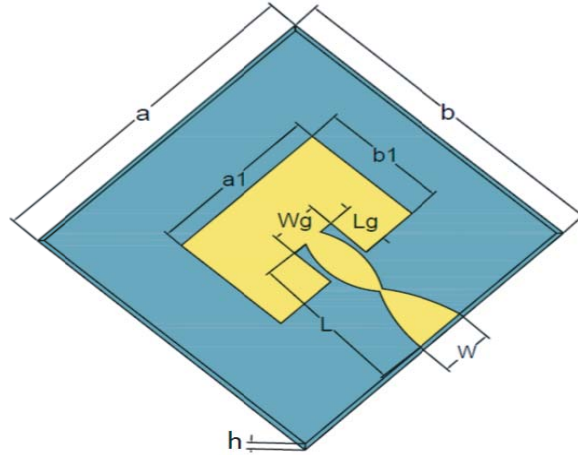


Figure 1. Configuration of the proposed non-uniform feed microstrip antenna.

Table 1. Dimensions of the proposed antenna (cm).

<i>a</i>	<i>b</i>	<i>a</i> ₁	<i>b</i> ₁	<i>h</i>	<i>L</i>	<i>Lg</i>	<i>Wg</i>
3.1	4.2	1.7	1.42	0.08	1.6	0.45	0.5

and characteristics are represented in Table 1. The dimension of the radiation patch is designed at a frequency of 5.5 GHz.

If the width of the transmission line is 1.66 mm and uniform, the impedance of the transmission line would be 50 ohms. The point at which the transmission line is connected to the patch is selected such that the microstrip patch’s impedance is 50 ohms. Therefore, this antenna resonates at a frequency of 5.5 GHz. In order to match with the other frequencies near its excited mode, the antenna’s impedance should be calculated at the other frequencies so that the proper transmission line can be designed. Values of impedances for changes of *Wg* and *Lg* are measured at 5.25, 5.5, and 5.75 GHz, and the impedance of the antenna for *Wg* = 5 mm is $Z_1^{PORT} = 4 + i39$, $Z_2^{PORT} = 50$ and $Z_3^{PORT} = 5 + i25$. The impedance achieved in HFSS is the impedance at the input port. In order to design the transmission line, the impedance of the radiated patch is required; thus the impedance obtained for a 50 Ω transmission line of 16 mm length at the input port is converted to the impedance at the antenna using Eq. (1). The impedance of the antenna at the mentioned frequencies is $Z_1^a = 2.8 - i15$, $Z_2^a = 52.75 - i0.8$, and $Z_3^a = 4.4 - i14$, respectively. A transmission line should be designed to convert the 50 Ω impedance of the coaxial cable to these impedances [20].

$$\frac{dZ_i}{dx} + j\beta \frac{Z_i^2}{Z(x)} - j\beta Z(x) = 0 \tag{1}$$

where constant $Z(x)$ is the line characteristic impedance which varies with the line length x and $j = \sqrt{-1}$. Let us write Z_i as the input impedance.

The width equation of the transmission line is presented in Eq. (2):

$$W(x) = a_0 + a_1 \cos\left(\frac{2\pi x}{0.008}\right) + a_2 \cos\left(\frac{4\pi x}{0.008}\right) + a_3 \cos\left(\frac{6\pi x}{0.008}\right) \tag{2}$$

According to the formulation reported in [21], the link between $W(x)$ and $Z(x)$ is:

$$Z(x) = \frac{\eta_0}{2\pi\sqrt{\epsilon_{eff}}} \ln \left[\frac{h \cdot a \left(\frac{w}{h}\right)}{w} + \sqrt{1 + \frac{4h^2}{w^2}} \right] \tag{3}$$

where

$$a\left(\frac{w}{h}\right) = 6 + (2\pi - 6) \cdot \exp\left[-\left(\frac{30 \cdot 66h}{w}\right)^{0.7528}\right] \quad (4)$$

with η_0 being the air impedance and ε_{eff} the effective permittivity of the medium.

Unknown coefficients of a_0 , a_1 , a_2 , and a_3 should be found so that the transmission line can be properly matched with the antenna. NMPC is used in order to find these coefficients. To find the coefficients for a different W , its impedances are calculated. Then the coefficients proportional to the minimum reflection coefficient are obtained.

3. NONLINEAR MODEL PREDICTIVE CONTROL

NMPC is one of the nonlinear control methods which can be used as a method of optimization. As mentioned above, it is used for optimization as a simple control approach for complex systems. Given the general form of Eq. (1) and the derivative part ($\frac{dz}{dx}$), using NMPC seems preferable to other optimization algorithms such as Genetic Algorithm (GA) and Invasive Weed Optimization (IWO). The main reason for this success is the MPC design's ability to deliver high-performance control systems that can operate for long periods of time without expert intervention.

It is possible to summarize the incredible benefits of this approach as follows:

- Precise prediction of future plant behaviour.
- The possibility of optimizing the current state by considering the future modes.
- Computing the requisite corrective control action required to bring the expected output as close to the desired target value as possible.
- Best for processes with a significant number of variables regulated and controlled.

NMPC is a digital controller, that is, a method of discrete time. Thus when computation of the control is accomplished using a digital computer and at each sampling time, the results are applied online. NMPC obtains a finite horizon open-loop optimal control problem subject to system dynamics and constraints. Here, we investigate model predictive control for nonlinear control and optimization systems of the form [22]

$$x(k+1) = f(x(k), u(k)) \quad x(0) = x_0 \quad (5)$$

where $x(k)$ and $u(k)$ are the system state and input vector at sampling place k , respectively. Also f is the NMPC equation which is defined in Eq. (6).

As previously mentioned, in a moving horizon approach, this procedure is repeated. The concept of the moving horizon is shown in Figure 2. Suppose that we are at the given sampling place k . The past output (Z) and input (u) patterns are known up to k and $k-1$, respectively. Therefore, the cost function tries to find those control actions that move the desired reference approach towards the future trend of the output. The control actions are found through iterations. The output and input constraints are also considered in the optimization problem. The first control action $u(k|k)$ is then chosen over the interval $[k, k+1]$ and applied to the real plant. In this method, (H_p) and (H_c) are the prediction and control horizons, respectively (over a control horizon $(H_c) \leq (H_p)$). The number of parameters used to obtain the subsequent control history is described by H_c , and the number of control steps used to optimize the objective function subject to $((H_c) \leq (H_p))$ is described by H_p . H_p dictates how 'far' we wish the future to be predicted. The MPC implementation is not limited to any specific type of model, but the selected template type greatly affects the implementation and computation criteria.

Since $Z_x = u$ (output) and $Z_i = x$, the state space equation is as follows:

$$f = x(k+1) = (x(k)) + \frac{L * j\beta}{k} [-x^2(k)/u + u(k)] \quad (6)$$

where β is the phase constant, and L is the length of the matching line.

The cost function, which is defined along the predicted horizon, should be minimized to calculate the optimal input of the plant as follows:

$$J = \sum_{f=5.25}^{5.75} \sum_{i=1}^{H_p} \left\| Z_i^f(k+i|k) - \hat{Z}^f(k) \right\|_Q^2 + \sum_{i=1}^{H_c-1} \left\| \Delta u(k+i|k) \right\|_R^2 \quad \text{for } k = 0, 1, \dots, K-1 \quad (7)$$

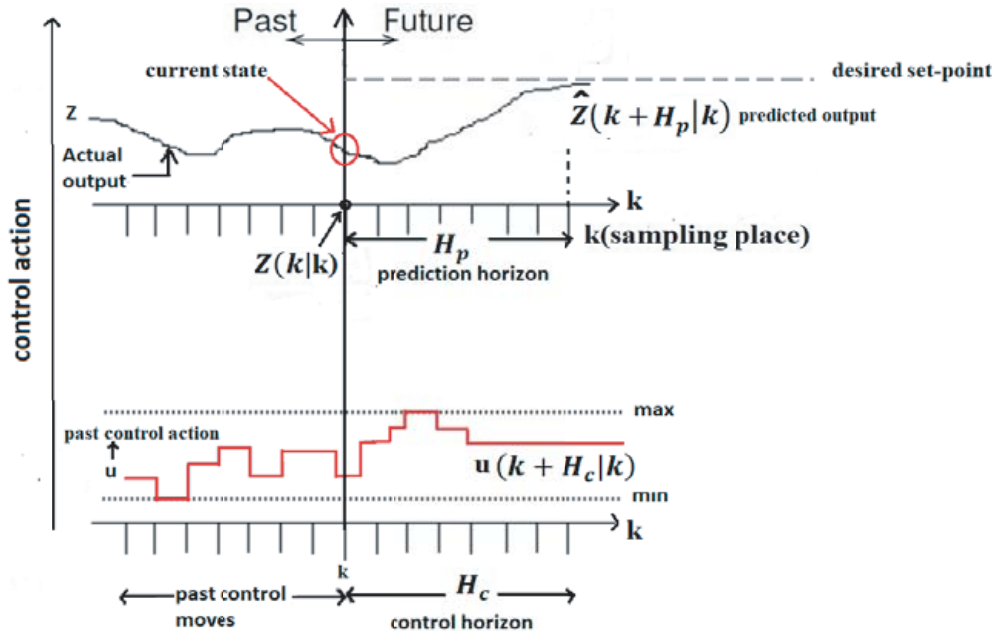


Figure 2. Receding horizon control scheme.

In the above, R and Q are constant weights. \hat{Z} is the predicted impedance, and $\Delta u(k), \Delta u(k+1), \dots, \Delta u(k+H_c-1)$ are the set of present and future incremental moves. As shown in Eq. (7), in which the second term represents the physical constraints on the input and its movement, the second term can be combined and formulated as constraints on the input movement and then added to the optimization problem. This treatment is more suitable because the cost function consequently contains only the input movements. Inputs are not optimized because they create steady state offsets. Also, it is obvious that for a feasible trajectory \hat{Z} , the NMPC leads to improvement over the offline optimization.

According to fabrication restrictions, the system constraints are as follows:

$$\begin{cases} u_{\min} \leq u \leq u_{\max} \\ x_{\min} \leq x \leq x_{\max} \end{cases} \quad (8)$$

Figure 3 shows impedance variation at frequencies of 5.25, 5.5, and 5.75 GHz along the transmission line based on the optimized coefficients.

The results obtained using MATLAB for coefficients of the nonuniform transmission line are presented in Table 2. Considering Eq. (1), with this coefficient, the reflection coefficients at 5.25, 5.5, and 5.75 GHz are 0.1, 0.3, and 0.13, respectively. The convergence time of model analysis and predictive control is 5 seconds.

Table 2. The cosine extension’s coefficient of the transmission line for wideband microstrip antenna for $W(x)$ based on millimeter.

a_0	a_1	a_2	a_3
0.5	-0.4	1.4	1.4

4. RESULTS

According to the dimensions of the patch and optimized transmission line, the proposed antenna and conventional antenna are simulated in HFSS. The proposed antenna is fabricated and shown in Figure 4. The measurement results are obtained using the HP8510 network analyzer and an anechoic chamber.

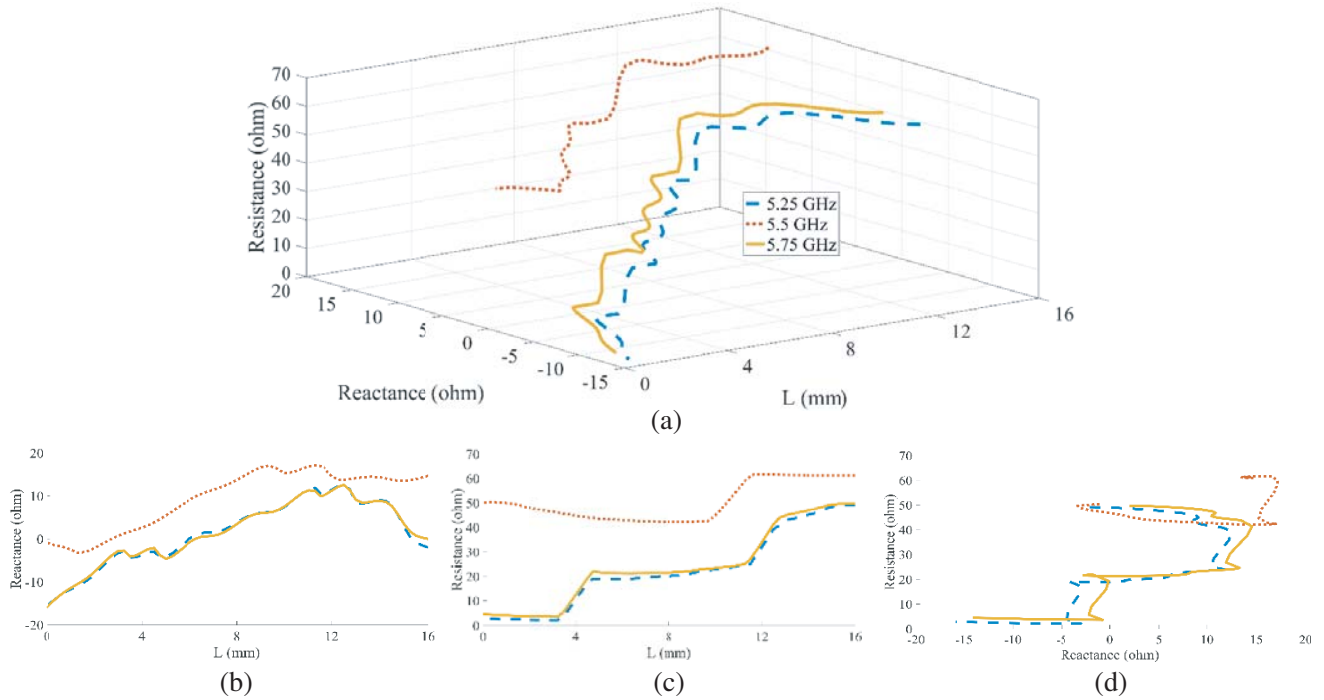


Figure 3. The impedance of the proposed non-uniform transmission line at 5.25, 5.5, and 5.75 GHz. (a) 3D view, (b) reactance at feed's length, (c) resistance at feed's length, (d) ratio between reactance and resistance.

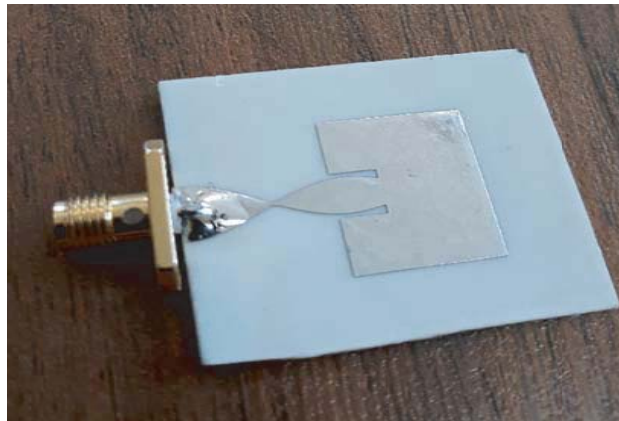


Figure 4. The fabricated proposed microstrip antenna.

Figure 5 shows the impedance value of the proposed antenna obtained from the HFSS software at the feed location.

Figure 6 shows the reflection coefficient of the conventional and proposed microstrip patch antenna. The structure in which the nonuniform transmission line is present results in a good impedance matching throughout the bandwidth of 5.15–5.85 GHz. The impedance bandwidth of the proposed nonuniform feed microstrip patch antenna is 13%, which is approximately four times greater than the conventional microstrip patch antenna. The radiation patterns of the antenna with a nonuniform transmission line at 5.25, 5.5, and 5.75 GHz are shown in Figure 7, where the cross polarization is 30 dB. The low cross polarization and stability of the pattern show that the impedance bandwidth is improved while the characteristics of antenna are preserved. The cross-polarization is -20 dB, -30 dB, and -40 dB at

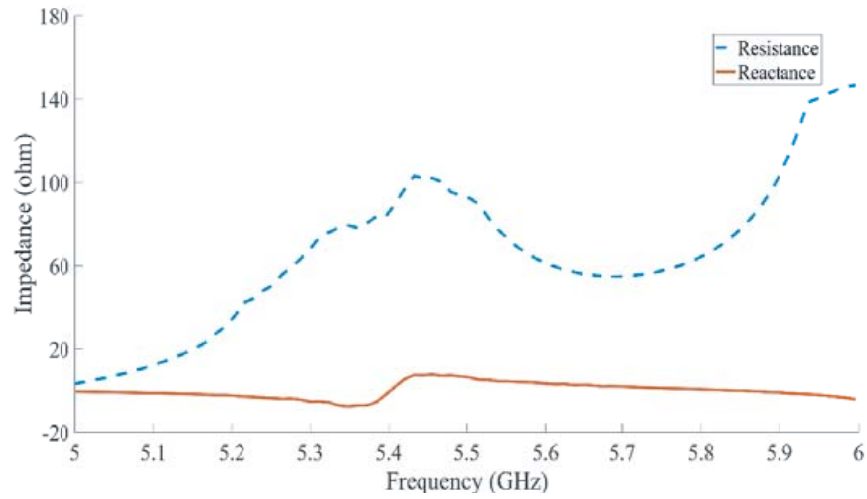


Figure 5. The impedance of the proposed microstrip patch antenna with non-uniform feed line.

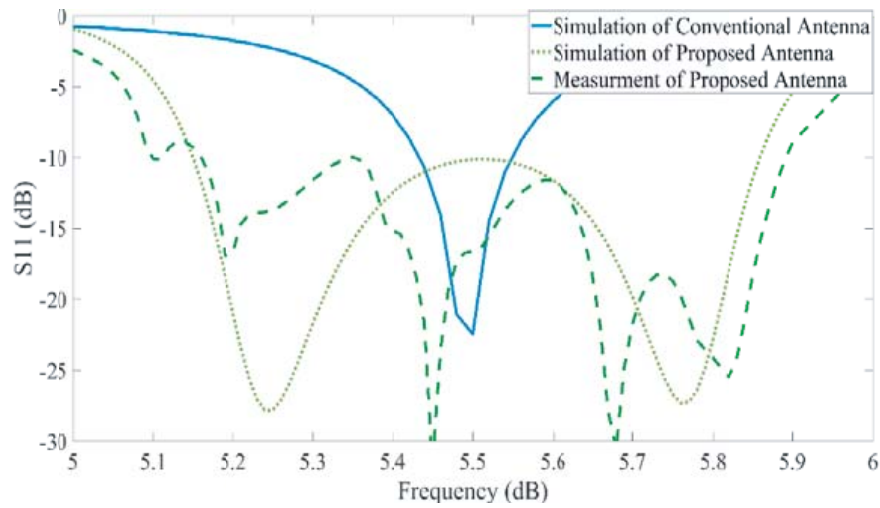


Figure 6. Reflection coefficient of the conventional and the proposed antenna.

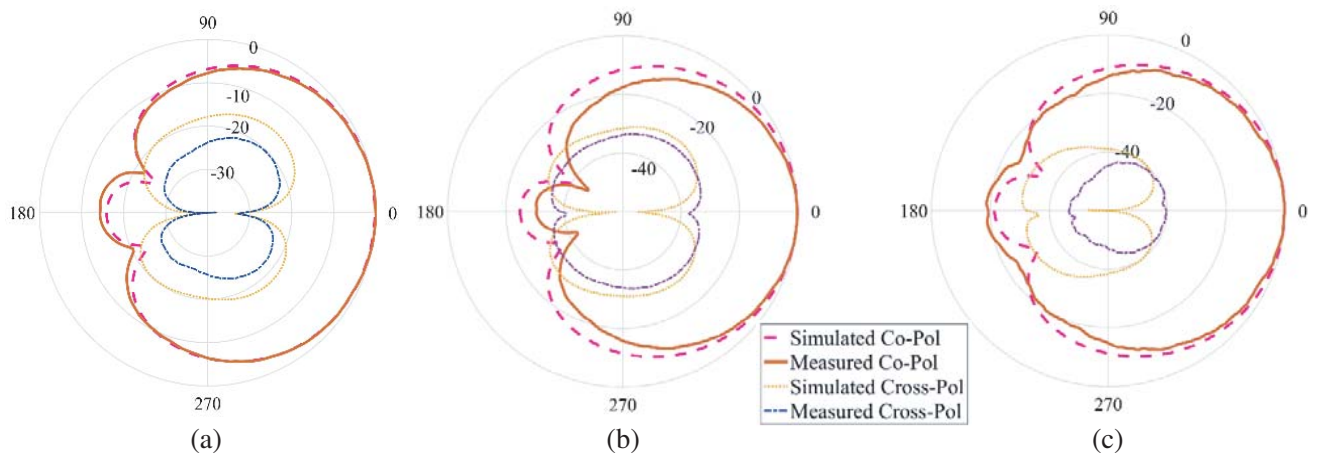


Figure 7. Radiation patterns of the non-uniform feed microstrip patch antenna at (a) 5.25 GHz, (b) 5.5 GHz, (c) 5.75 GHz.

the frequencies of 5.25 GHz, 5.5 GHz, and 5.75 GHz, respectively. Moreover, the back lobe is -15 dB, -25 dB, and -20 dB at the above-mentioned frequencies, respectively.

As can be seen in these figures, the simulation and measurement results are in good agreement with each other. The mean peak gain and efficiency at the frequency bandwidth are 6.5 dBi and 89%, respectively.

5. CONCLUSION

In this paper, NMPC is used to design a microstrip antenna. A transmission line is presented to match the 50-ohm impedance of the coaxial cable with the complex impedances of the microstrip patch at different frequencies. Using the impedance variation equation of the transmission line as the dynamic equation of the NMPC, the unknown coefficients of the nonuniform transmission, which are extended in cosine form, are calculated. This transmission line provides a minimum reflection coefficient at the frequency bandwidth. The proposed antenna provides 13% bandwidth at the central frequency of 5.5 GHz. Therefore, the simulation and measurement results show the proposed method's high performance.

REFERENCES

1. Rabobason, Y. G., G. P. Rigas, S. Swaisaenyakorn, B. Mirkhaydarov, B. Ravelo, M. Shkunov, P. R. Young, and N. Benjelloun, "Design and synthesis of flexible switching 1×2 antenna array on Kapton substrate," *Eur. Phys. J. Appl. Phys. (EPJAP)*, Vol. 74, No. 3, 1–10, 2016.
2. Rabobason, Y. G., G. P. Rigas, S. Swaisaenyakorn, B. Mirkhaydarov, B. Ravelo, M. Shkunov, P. R. Young, and N. Benjelloun, "Design of flexible passive antenna array on Kapton substrate," *Progress In Electromagnetics Research C*, Vol. 63, 105–117, 2016.
3. Cheng, B., Z. Du, and D. Huang, "A broadband low-profile multimode microstrip antenna," *IEEE Antennas and Wireless Propagation Letters*, Vol. 18, No. 7, 1332–1336, July 2019.
4. Tiwari, R. N., P. Singh, and B. K. Kanaujia, "Butter fly shape compact microstrip antenna for wideband applications," *Progress In Electromagnetics Research Letters*, Vol. 69, 45–50, 2017.
5. Wi, S., Y. Lee, and J. Yook, "Wideband microstrip patch antenna with U-shaped parasitic elements," *IEEE Transactions on Antennas and Propagation*, Vol. 55, No. 4, 1196–1199, April 2007.
6. Cao, Y., et al., "Broadband and high-gain microstrip patch antenna loaded with parasitic mushroom-type structure," *IEEE Antennas and Wireless Propagation Letters*, Vol. 18, 1405–1409, 2019.
7. Weigand, S., G. H. Huff, K. H. Pan, and J. T. Bernhard, "Analysis and design of broad-band single-layer rectangular U-slot microstrip patch antennas," *IEEE Transactions on Antennas and Propagation*, Vol. 51, No. 3, 457–468, March 2003.
8. Liu, S., W. Wu, and D. Fang, "Single-feed dual-layer dual-band E-shaped and U-slot patch antenna for wireless communication application," *IEEE Antennas and Wireless Propagation Letters*, Vol. 15, 468–471, 2016.
9. Li, M. and K. Luk, "A differential-fed UWB antenna element with unidirectional radiation," *IEEE Transactions on Antennas and Propagation*, Vol. 64, No. 8, 3651–3656, August 2016.
10. Islam, M. T., M. N. Shakib, and N. Misran, "Design analysis of high gain wideband L-probe fed microstrip patch antenna," *Progress In Electromagnetics Research*, Vol. 95, 397–407, 2009.
11. Klionovski, K. and A. Shamim, "Physically connected stacked patch antenna design with 100% bandwidth," *IEEE Antennas and Wireless Propagation Letters*, Vol. 16, 3208–3211, 2017.
12. Sharma, R., A. Kandwal, and S. K. Khah, "Wideband DGS circular ring microstrip antenna design using fuzzy approach with suppressed cross-polar radiations," *Progress In Electromagnetics Research C*, Vol. 42, 177–190, 2013.
13. Wong, H., K. K. So, and X. Gao, "Bandwidth enhancement of a monopolar patch antenna with V-shaped slot for car-to-car and WLAN communications," *IEEE Transactions on Vehicular Technology*, Vol. 65, No. 3, 1130–1136, March 2016.

14. Liu, N., L. Zhu, W. Choi, and X. Zhang, "A low-profile aperture-coupled microstrip antenna with enhanced bandwidth under dual resonance," *IEEE Transactions on Antennas and Propagation*, Vol. 65, No. 3, 1055–1062, March 2017.
15. Lu, W., Q. Li, S. Wang, and L. Zhu, "Design approach to a novel dual-mode wideband circular sector patch antenna," *IEEE Transactions on Antennas and Propagation*, Vol. 65, No. 10, 4980–4990, October 2017.
16. Pozar, D. M., *Microwave Engineering*, John Wiley & Sons, 2011.
17. Khalaj-Amirhosseini, M., "Wideband or multiband complex impedance matching using microstrip nonuniform transmission lines," *Progress In Electromagnetics Research*, Vol. 66, 15–25, 2006.
18. Jin, T., H. Wei, D. L. M. Nzongo, and Y. Zhang, "Model predictive control strategy for NPC grid-connected inverters in unbalanced grids," *Electronics Letters*, Vol. 52, 1248–1250, 2016.
19. Novak, M., U. M. Nyman, T. Dragicevic, and F. Blaabjerg, "Analytical design and performance validation of finite set MPC regulated power converters," *IEEE Transactions on Industrial Electronics*, Vol. 66, 2004–2014, March 2019.
20. Ajose, S. O., "Design formulas for impedance matching using a Hermite line," *IEE Proceedings H — Microwaves, Antennas and Propagation*, Vol. 133, 319–320, August 1986.
21. Eudes, T., B. Ravelo, and A. Louis, "Transient response characterization of the high-speed interconnection RLCG-model for the signal integrity analysis," *Progress In Electromagnetics Research*, Vol. 112, 183–197, 2011.
22. Grüne, L. and J. Pannek, *Nonlinear Model Predictive Control*, Springer International Publishing AG, Switzerland, 2017.